Lossy Data Compression of Vibrotactile Material-Like Textures

Shogo Okamoto, *Member*, *IEEE*, and Yoji Yamada, *Member*, *IEEE*

Abstract—Tactile content will be delivered over the Internet in the near future. Vibrotactile material-like textures that resemble the surfaces of wood, leather, etc., are representative of such content. We performed lossy compression of texture data for reducing the data size. We confirmed the effectiveness of two compression strategies: quantization and truncation of data beneath a shifted perceptual threshold curve. In the quantization strategy, the amplitude spectra of vibrotactile textures could be quantized in 14 steps. This reduced the data size to approximately one quarter without any noticeable quality deterioration. The method for truncating frequency components with amplitudes smaller than a shifted perceptual threshold curve was also effective, and it was preferable to the automatic deletion of subthreshold amplitudes. We reduced the data size of vibrotactile material textures to 10-20 percent of their original size by combining the lossy data compression strategy with Huffman coding, which is a lossless data compression method. Lossy compression algorithms will enhance the online delivery of vibrotactile material-like textures by decreasing their data size without significant loss of quality.

Index Terms—Vibrotactile texture, quantization, threshold

1 Introduction

Tactile content will be delivered over the Internet in the near future via tactile displays installed on computer mice or mobiles. Such devices are already being developed commercially, for example, iFeel MouseMan from Logitech, Tangible Mouse from Fuji Xerox, and Orbit 3D by Kensington. Tactile content will be based on stimulation techniques that have been studied by many researchers. These techniques include the presentation of textures such as roughness (e.g., [1], [2], [3], [4], [5]), virtual mechanical switches, buttons or slide bars (e.g., [6], [7], [8], [9]), iconic tactile stimuli [10], [11], contact with objects [12], [13], and affective or social communication [14], [15]. With the amount of tactile content increasing, data compression methods are potentially effective for the delivery of such tactile content through the Internet.

In this study, we address lossy data compression of tactile textures. Textures have a large data size compared with virtual mechanical switches or iconic tactile stimuli because they are spatially distributed on the surfaces of objects. We consider material-like textures with irregular surface patterns, rather than simple textures such as gratings. An evident contribution of data compression is the reduction of communication traffic. Moreover, it can potentially contribute to the understanding of new aspects of tactile perception. From the history of data compression for visual and auditory signals, it can be seen that the development of compression algorithms leads to the investigation of human perceptual mechanisms from the viewpoint of data compression because compression algorithms exploit such perceptual characteristics. Conventionally, researchers investigating tactile perception did not consider compression algorithms; many of them attempted to create guidelines for haptic interfaces. Hence, data compression techniques are expected to inspire studies on new aspects of tactile perception that are related to data compression.

While it is probable that data compression methods used for sounds or images [16] will be applicable to tactile textures, there have been no previous reports on the use of such methods; therefore, the extent to which textures can be compressed is unknown. Some of the compression methods used for sounds or images truncate information that is irrelevant for the requisite qualities; hence, we need to clarify whether truncations are appropriate for tactile textures. The objectives of this study are to test the applicability of lossy data compression algorithms to vibrotactile material-like texture data and to investigate their suitability in terms of potential data reduction ratios. We employ two types of fundamental compression algorithms, namely, quantization and truncation of subthreshold data. These will be elaborated in Section 4.3.

We consider vibrotactile stimuli that are commonly used for tactile displays. Although a variety of vibrotactile displays are available, we use a display with a single vibratory source known as a "contactor" or "tactor." This type of display is the most fundamental, and a single contactor would be preferable in commercial products because it would reduce costs. For example, vibrotactile displays with a single contactor were used in [5], [6], [7], [13], [14]. In contrast, vibrotactile displays with multiple actuators have also been represented by pin matrices in [1], [2], [4], [17], and a shearing stress display in [18].

The current study is an extension of our previous study [19], where we tested the use of lossy data compression

• *The authors are with the Department of Mechanical Science and Engineering, Graduate School of Engineering, Nagoya University, Room 302, 2nd Build. of School of Engineering, Furo-cho, Chikusa-ku, Nagoya, Japan. E-mail: {okamoto-shogo, yamada-yoji}@mech.nagoya-u.ac.jp.*

Manuscript received 23 Sept. 2011; revised 21 Mar. 2012; accepted 28 Mar. 2012; published online 18 Apr. 2012.
Recommended for acceptance by H.Z. Tan.
For information on obtaining reprints of this article, please send E-mail to: toh@computer.org, and reference IEEECS Log Number TH-2011-09-0074.
Digital Object Identifier no. 10.1109/ToH.2012.18.

algorithms for two types of vibrotactile textures. To preserve the generality of the algorithms in the current study, we use three types of material-like textures with new experimental participants. Then, we combine the compression algorithm with Huffman coding, which is a lossless compression scheme, in order to estimate the potential compression ratios of vibrotactile material-like texture data.

2 Related Work

Data compression algorithms are divided into lossy or lossless schemes, and this study considers the former case. Lossless schemes such as Huffman coding reduce the size of data by making use of the stochastic properties of signals. Data compressed by using lossless schemes are decoded into exactly the same form as that of the original data. In contrast, lossy schemes utilize human perceptual properties to convert the original data into a form that is perceptually close or identical to the original data. The current study is concerned with lossy data compression schemes.

Compression technologies used for multimedia information are useful for compressing tactile texture data. Here, we introduce sound and image compression schemes that are of relevance to the methods used in this study. We also review studies of haptic information compression.

2.1 Quantization and Elimination of Subthreshold Signals

A fundamental strategy in lossy data compression is quantization. Small quantization errors do not influence the subjective quality. Quantization has been introduced in various compression algorithms. One such algorithm is JPEG, which is a compression technique for still pictures [16]. JPEG technology computes the discrete cosine transformation (DCT) of a picture in order to extract the intensities of individual spatial frequencies (DCT coefficients). The extracted DCT coefficients are quantized using step sizes that are specific for individual frequency ranges, based on human luminosity characteristics. Lossless schemes such as differential or Huffman encoding are then applied to the quantized data. In some cases, people cannot distinguish the original images from those compressed to one tenth of the data size [20], [21]. One of the methods in this study also employs DCT and quantization (see Sections 4.3.1 and 4.3.2).

Another fundamental strategy is the truncation of signals beyond perceptual thresholds. An example of this method is MPEG audio encoding [16], where sound components below perceptual thresholds are removed during encoding. Masking thresholds specified for individual critical bands are also employed during encoding. We also adopt a strategy for removing frequency components with amplitudes below certain thresholds (see Section 4.3.3).

2.2 Lossy Data Compression in Haptics

Data compression of force or position information was studied in order to reduce data transfer in haptic systems such as a remote master-slave system. Hinterseer et al. [22], [23], and Nitsch et al. [24], [25] transferred force or position information to the operators of their haptic systems only when information or changes in information exceeded certain thresholds or discrimination limens, respectively. Shahabi et al. [26] proposed the compression of force and position data using a variable sampling method or adaptive differential pulse-code-modulation. You and Sung [27] and Kuschel et al. [28] used predictive coding methods to decrease the data transfer in a master and slave system. Jensen et al. attempted to reduce the data sizes of voxels by clipping the data around an end effector, which was intensively refreshed [29]. Jensens method is similar to a speedup technique used in haptic rendering rather than data compression methods. Arimoto et al. investigated the effects of position data quantization on subjective quality during haptic manipulation of virtual objects [30]. Borst compared the uniform and nonuniform quantization of force data using a force display and suggested the superiority of the nonuniform scheme [31]. The concepts of the quantization of stimuli data and the removal of subliminal data found in these schemes are common to the compression methods used for tactile textures in the current study.

Data compression of force and position feedback has already been attempted in haptics; however, the compression of tactile stimuli data has not been conducted extensively. A similar study on the compression of textile stimuli was reported by Cholewiak et al. [32], where square gratings were decomposed into major waves and harmonics using Fourier expansion. The effects of harmonics on the perceptual thresholds of gratings were then investigated, before proposing the thresholds of fine or midcoarse square gratings based on the thresholds of their major waves. This suggests that the high-frequency harmonic components of square gratings can be ignored to some extent during the presentation of vibrotactile textures. The study also suggested that it was possible that humans did not perceive changes in the phases between two sinusoidal waves when the synthetic waves of these two waves were presented. This suggests that the phase information of vibrotactile texture stimuli can be partially removed. Phase information is particularly unnecessary during the synthesis of high-frequency vibrotactile stimuli [33]. However, it is evident that few studies have reported the use of lossy data compression for tactile textures. This may be partly because the simultaneous manipulation of a large number of physical variables such as the vibrotactile amplitudes in many frequency bands is rarely addressed in psychophysics, which is a highly sophisticated discipline that investigates the perception of physical stimuli. We use a simple experimental design, which is described later; it allows us to handle such stimuli that involve changes in many physical variables.

3 Equipment

3.1 Vibrotactile Texture Display

We used a vibrotactile display with one vibratory source. The display should enable the users to move their hands and actively explore spatially distributed textures. We used the vibrotactile display shown in Figs. 1a and 1b; it satisfies the points stated above.

The vibrotactile stimulator was a piezo-stack actuator (NEC/TOKIN, AHB800C801FPOLF, Sendai, Japan) that was installed on a low-friction linear slider (SS series, NSK,

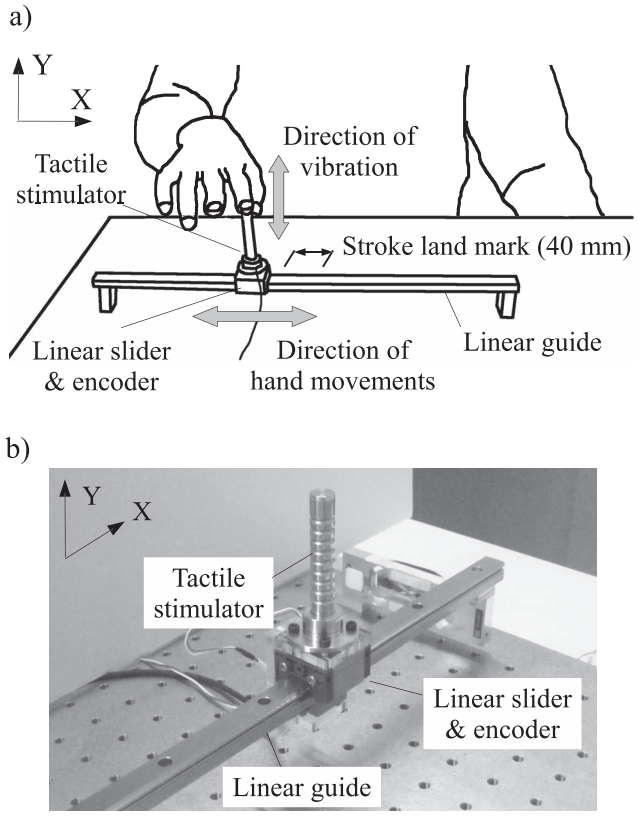

Fig. 1. Experimental setup. a) Use of the vibrotactile display. b) Linear slider type vibrotactile display.

Tokyo, Japan; average friction measured with a typical load of 200 g was 0.10 N). The sliders position on the guide was measured using an optical linear encoder (SR-P1000, Canon, Tokyo, Japan) with the resolution set at $0.4\ \mu\mathrm{m}$. When a participant in the experiments placed his/her finger on the vibrator and moved his/her hand along the X-axis, the vibrator slid along the guide and produced displacements along the Y-axis that reproduced the surface profile of the texture. The contactor was circular with a diameter of 11.6 mm. The refresh rate for the voltage output to the vibrator was 3.0 kHz.

The output force of the stimulator was approximately 800 N, which was sufficiently large compared with the force applied by the finger to prevent the latter from causing the output displacements to decay. Thus, feedback control was not required to ensure set displacements. The maximum output displacement of the stimulator was approximately $80\ \mu\mathrm{m}$ with an applied voltage of 150 V. The displacement changed linearly with the input voltage when the frequency was fixed. The frequency response curve was relatively flat and it did not exhibit resonance in the range used in the experiments (up to 400 Hz). The frequency response magnitude curve reached -3 dB at 270 Hz. To compensate for attenuation at high frequencies and ensure that the desired displacements were output, the voltage inputs to the stimulator were multiplied by the inverse function of the frequency response curve. Voltage was applied to the stimulator through a bipolar amplifier (FRA5014, NF, Yokohama, Japan, nominal frequency response was 2 MHz).

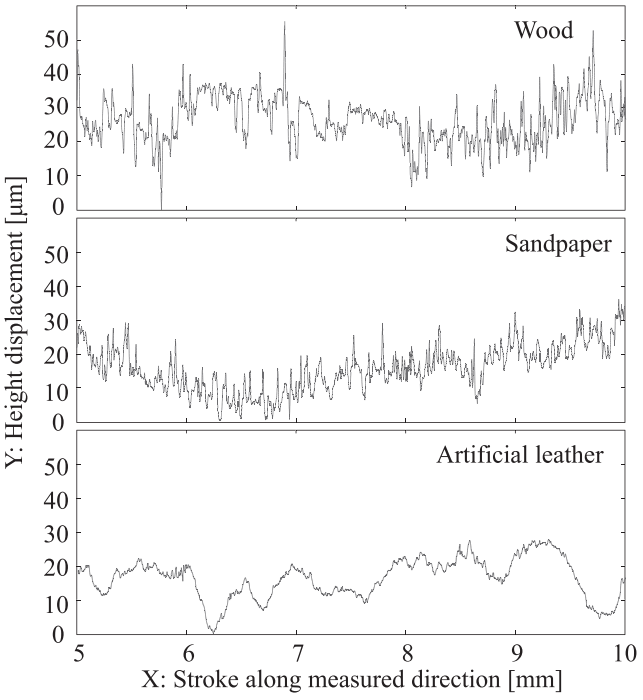

Fig. 2. Surface profiles of material textures.

3.2 Material-Like Texture

We used material-like textures with irregular surface height patterns. We measured the surface roughness profiles of 11 materials, including wood, paper, and cloth. A noncontact surface measurement method (NH-3SP, Mitaka Kohki, Mitaka, Japan; nominal resolution of 1 nm) was used to measure the surface profiles. It measured the surface of a randomly selected portion of each texture for 10 mm with an interval of $0.5\ \mu\mathrm{m}$. Different types of textures were used to ensure the generality of the effects of the compression algorithms. We played back the 11 measured material textures using the above tactile display and we selected three materials that felt obviously different. These were a board made from the wood of a Judas tree, a piece of sandpaper (#1,500), and a piece of artificial leather (DI-NOC Film, LE-137, 3M). The measured profiles of these textures are shown in Fig. 2. We displayed these profiles as height variations to human finger pad. Note that these variations do not exactly match those experienced while stroking real materials. Hence, these textures are called material-like textures.

4 Lossy Data Compression Algorithms

4.1 Perceptual Characteristics of Vibrotactile Stimuli

Compression methods exploit the discriminability and detectability characteristics of specific amplitudes found in vibrotactile stimuli. The discriminability indicates how supraliminal stimuli should be treated. A typical index for discriminability is the differential threshold, which has a Weber ratio of 10-20 percent (computed from [34] and [35]) when used for vibratory amplitudes. This indicates that amplitudes can be somewhat coarsely quantized. The detectability indicates how to handle subliminal stimuli. Subliminal vibrotactile stimuli need not be delivered to

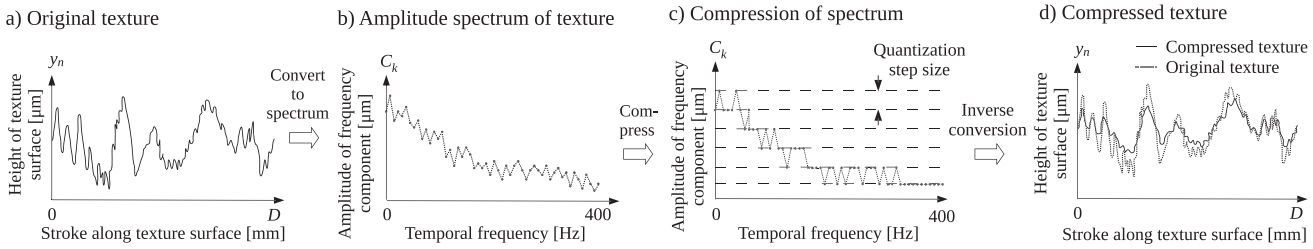

Fig. 3. Process flow for the compression of vibrotactile material textures.

users; hence, the compression algorithm eliminates amplitudes below the detection threshold. These two properties of vibrotactile stimuli have been discussed in terms of frequency space, and it is known that the quality of stimuli can be expressed in frequency space, such as power spectra [36], [37], [38]. Thus, the compression of material textures was also performed in frequency space in this study.

4.2 Data Compression Using Discrete Cosine Transformation

Fig. 3 shows the process of data compression. First, the textures surface profiles (Fig. 3a) are converted into amplitude spectra using a discrete cosine transformation (Fig. 3b) and data compression algorithms are then applied to the spectra (Fig. 3c). Finally, the modified or compressed spectra are converted into a surface profile using inverse DCT (Fig. 3d). Although we measured material surfaces for 10 mm, the generated surface profiles repeated this procedure for a virtually infinite material length. Each of these processes is described in detail in the following sections.

Samples of the textures height $y_n(n = 0, \ldots, N-1)$, which are measured as described in Section 3.2, are converted into amplitude spectra $C_k(k = 0, 1, \ldots, N-1)$, where N is the number of samples ($N = 20{,}000$) and C_k is the amplitude of the frequency component f_k. The DC component C_0 was set to zero because it does not influence perception. Components with frequencies higher than 400 Hz were removed when the texture was explored at a typical hand velocity $\overline{v}$. This velocity was set to encompass a range where natural explorations were not disturbed (50 mm/s). In the experiments described below, participants conducted their explorations according to the rhythm of a metronome, and they used a specified stroke length to maintain an average velocity (as described in Section 5.2). Based on $\overline{v}$, f_k is determined by

$$f_k = \frac{\text{Sampling frequency}}{\text{Number of samples}} \cdot k = \frac{N/D \cdot \overline{v}}{N} \cdot k = \frac{\overline{v} \cdot k}{D}, \qquad (1)$$

where D is the distance over which the texture surface was measured (10 mm). N/D is equivalent to the number of sampling events per millimeter.

4.3 Data Compression Algorithms for Vibrotactile Textures

4.3.1 Linear Quantization

Quantization is one of the most popular strategies for lossy data compression. The amplitudes are quantized between the maximum and minimum C_k. The quantized amplitude spectrum L_k is determined by

$$L_k = \text{round}\left(\frac{C_k}{\Delta}\right) \cdot \Delta, \qquad (2)$$

where Δ is the quantization step. Δ is given as

$$\Delta = \frac{\max(C_1, \ldots, C_{N-1}) - \min(C_1, \ldots, C_{N-1})}{L - 1}, \qquad (3)$$

where L is the number of quantization steps, which determines the compression level. Fig. 4 shows an example of amplitude spectra and the surface profile of uncompressed and linearly quantized ($L = 4$) wood textures. Given that each amplitude of the uncompressed texture was written in 2 bytes, the data size of the compressed texture in the figure was 12.5 percent of the size of the uncompressed data. Here, the compression ratio is defined as

$$\text{Compression ratio} = \frac{\text{Data size of compressed texture}}{\text{Original data size}}. \qquad (4)$$

4.3.2 Log Quantization

There are two types of quantization schemes: uniform and nonuniform quantization. The step size is constant in uniform quantization schemes, whereas the step size varies in nonuniform schemes. An example of a nonuniform

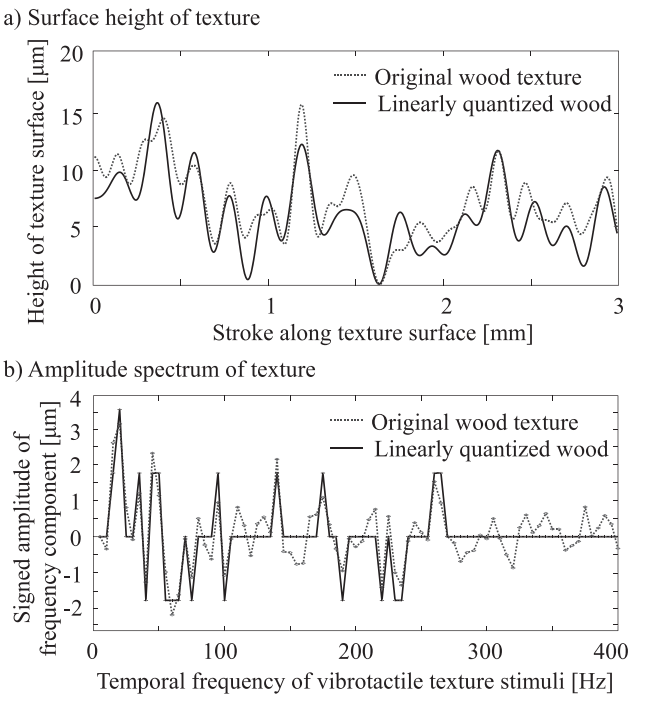

Fig. 4. Linearly quantized wood texture: $L = 4$.

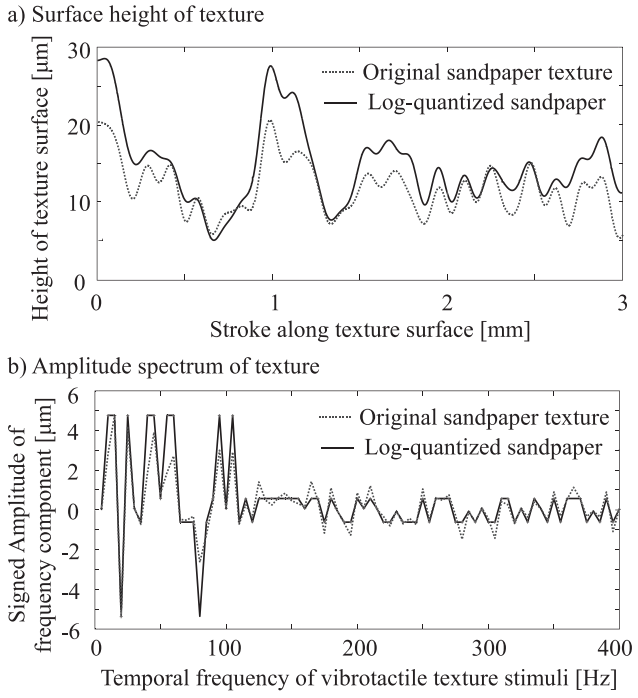

Fig. 5. Log-quantized sandpaper texture: $L = 6$.

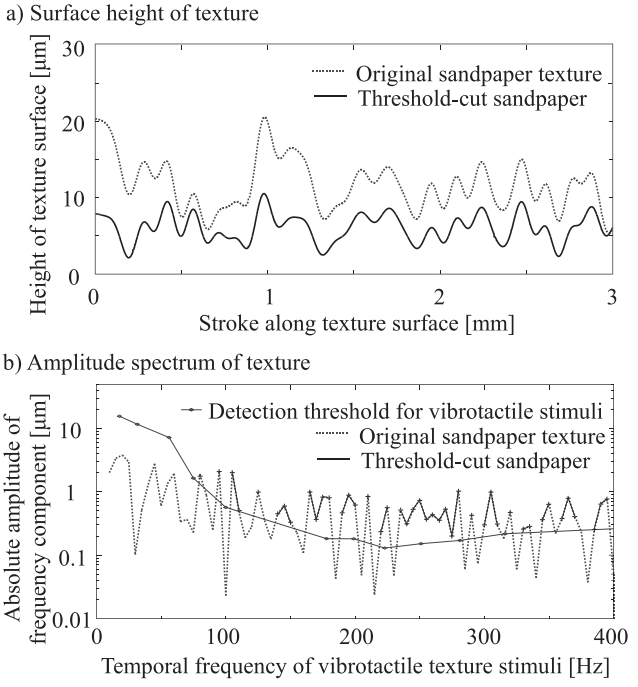

Fig. 6. Sandpaper texture with truncation of amplitudes below $\log_{10} b(F) + b_0|_{b_0=0}$.

scheme is log pulse-code-modulation where the step size varies logarithmically. Low-level signals are finely quantized; thus, quantization errors become small. In contrast, high-level signals are coarsely quantized.

The application of fine quantization steps to low amplitudes and coarse quantization steps for high amplitudes is expected to effectively reduce the data size, while maintaining data quality by taking into account Webers law. We used a log function to determine the step sizes. Positive and negative amplitude values were quantized separately. With a positive C_k, the log-quantized amplitude N_k is determined by

$$\log_{10} N_k = \mathrm{round}\left(\frac{\log_{10} C_k - \log_{10} S}{\Delta^+}\right) \cdot \Delta^+ + \log_{10} S \quad (5)$$

$$\text{if } C_k > S\ \Delta^+ = \frac{\max(\log_{10} C_k | C_k > 0) - \log_{10} S}{L/2 - 1}. \quad (6)$$

With a negative C_k, N_k is determined by

$$\log_{10} N_k = \mathrm{round}\left(\frac{\log_{10}(-C_k) - \log_{10} S}{\Delta^-}\right) \cdot \Delta^- + \log_{10} S \quad (7)$$

$$\text{if } C_k < -S\ \Delta^- = \frac{\max(\log_{10} -C_k | C_k < 0) - \log_{10} S}{L/2 - 1}. \quad (8)$$

The amplitudes are quantized between the maximum or minimum C_k and S. S is a very small amplitude that hardly influences the perceived texture (here, $0.05\ \mu$m). For C_k with an amplitude lower than S, N_k is determined by

$$N_k = \mathrm{sign}(C_k) \cdot S \quad \text{if} \quad |C_k| \le S. \quad (9)$$

Clearly, S affects the performance of the compression algorithm. S needs to be sufficiently small, but quantization errors increase if it is too small. An accurate determination of S will be achieved in future work.

Fig. 5 shows an example of a log-quantized sandpaper texture and its amplitude spectrum. The amplitudes were quantized in six steps. Larger amplitudes were quantized more coarsely. The data compression ratio of the texture shown in Fig. 4 was 16.2 percent.

4.3.3 Truncation of Data beneath Shifted Thresholds

Assuming that stimuli below the detection threshold level can be removed while still maintaining the perceptual quality of textures, a third compression method is used to eliminate vibratory amplitudes that are smaller than the thresholds. When they are removed, the amplitude spectra are determined by

$$T_k = \begin{cases} 0 & \text{if } \log_{10} C_k < \log_{10} b(F) + \dfrac{b_0}{20} \\ C_k & \text{otherwise,} \end{cases} \quad (10)$$

where $b(F)$ and b_0 are the detection thresholds at frequency F and a variable for shifting the threshold curve, respectively. b_0 determines the compression level of the method. For example, amplitudes smaller than the threshold curve are truncated when $b_0 = 0$ dB. When $b_0 = -2$ dB, amplitudes smaller than the -2-dB shifted threshold curve are truncated. With the latter value, the compression ratio was worse than with $b_0 = 0$ dB. The function $b(F)$ was initially acquired using a psychophysical method of adjustment involving six participants, with the same equipment used in this study. $b(F)$ was acquired while the hand remained still.

Fig. 6 shows the sandpaper texture compressed using this method, when $b_0 = 0$ dB. Fig. 6b shows that the compressed texture included no amplitudes lower than the threshold curve. In this example, 45 percent of the amplitudes were truncated and assigned as zero. This

algorithm alone did not reduce the data size of the texture. However, the algorithm influences the efficiency of the lossless data-compression algorithms because it affects the statistical properties of the amplitudes. Using this algorithm will result in more highly efficient compression using Huffman coding or other methods because the number of zero values in the amplitude signals increases.

5 Experiment: Subjective Comparison of Compressed Textures

5.1 Subjective Quality Measurement Compatible with International Telecommunication Union (ITU)-R

For subjective quality assessment of compressed textures, we use a grading scale based on the recommendations of the International Telecommunication Union. ITU standardized the methods for subjectively assessing the impairment of audio-visual content. Such impairment is caused by lossy data compression, poor decoding, electromagnetic disturbance, etc. ITU-R BT.500-12 (Methodology for the subjective assessment of the quality of television pictures) [39] recommends the usage of grading scales such as the one used in our study, or continuous quality-rating scales like a numerical scale. These methods are advantageous in that they allow assessors to retain both subliminal threshold levels and quality impairment curves. Subliminal thresholds indicate the best compression levels that do not involve significant quality degradation. On the other hand, the quality impairment curves indicate the quality impairment over the thresholds. In general, subliminal threshold levels and quality impairment curves are useful for the practical implementation of data compression.

Although the ITU-R methods are well accepted in industry, they are not as rigorous as well-established psychophysical methods (e.g., [40]). For example, the use of adjectives such as "possibly the same" and "possibly different" are prone to variable interpretations by participants and can be susceptible to response biases. We therefore collected additional data with two participants using a signal detection paradigm to verify the experimental results.

5.2 Tasks and Participants

Overview. The participants scored the subjective dissimilarity between the uncompressed and compressed textures. They rated the dissimilarity using a four point grading scale. Three types of algorithms were applied to the wood and sandpaper texture data. Linear quantization and truncation of subthreshold stimuli was applied to the surface of the artificial leather texture data, but not the log quantization algorithm. This was because log quantization produced similar performance to linear quantization with the wood and sandpaper textures [19]. Thus, we focused on the two methods other than the log quantization with the leather texture.

Tasks. In each trial, participants explored and compared the uncompressed and compressed textures using the vibrotactile texture display described in Section 3.1. In each trial, all textures were presented to the participants for a period of 5 s. To maintain an average hand velocity of 50 mm/s (see Section 4.2), participants moved their hands in strokes of 40 mm following the rhythm of a metronome (1.25 Hz) with a pattern of one stroke per beat. Marks on the desk indicated the stroke distance (Fig. 1a). During the exploration of two textures in each trial, participants were required to maintain finger contact status with the contactor. Participants recorded their answers after exploring the two textures. The participants manually recorded the texture similarity as "same," "possibly the same," "possibly different," or "different" on an answer sheet.

TABLE 1
Compression Level of Textures Used for Evaluation

Texture	Comp. algorithms	Compression levels
Wood	Lin. quant. [step]	$L = 14, 12, 10, 8, 6, 5, 4$
	Log quant. [step]	$L = 14, 12, 10, 8, 6$
	Threshold-cut [dB]	$b_0 = -12, -8, -4, 0, 4, 8$
Sandp.	Lin. quant. [step]	$L = 14, 12, 10, 8, 6, 5, 4$
	Log quant. [step]	$L = 14, 12, 10, 8, 6$
	Threshold-cut [dB]	$b_0 = -12, -8, -4, 0, 4, 8, 12$
Leather	Lin. quant. [step]	$L = 14, 12, 10, 8, 6, 5, 4$
	Threshold-cut [dB]	$b_0 = -12, -8, -4, 0, 4, 8, 12$

Test stimuli. The texture compression levels were set at 5-7 grades with each compression method. In addition to the compressed textures, uncompressed textures were included as test stimuli. Table 1 shows the compression levels used in the experiments for each type of texture. Each test stimulus was presented four times in total. For the wood texture, 76 trials were performed in total (19 textures $\times$ four repetitions) for each participant. For the sandpaper texture, 80 trials were performed (20 textures $\times$ four repetitions). For the artificial leather texture, 60 trials were performed (15 textures $\times$ four repetitions). The order of test stimuli presentation was random.

Participants. The participants were 15 university students who were recruited and paid according to methods approved by the ethics committee of the Engineering School of Nagoya University. Each participant sampled two textures of the three; thus, each type of texture was evaluated by a total of 10 participants. A specific participant conducted the experimental tasks with one type of the texture then, after a short break, they evaluated another type of the texture. The order of texture presentation was balanced. The participants listened to pink noise through noise-cancellation headphones to eliminate the sounds generated by the stimulator.

5.3 Results

Wood. Fig. 7 shows the means and standard deviations of the dissimilarity scores between the quantized and uncompressed wood textures. The standard deviations were calculated among participants. The values in the figure were computed by assigning a value of 0, 1, 2, or 3 to "same," "probably the same," "probably different," and "different," respectively. In general, the dissimilarity score increased (similarity decreased) as the data size of the compressed textures decreased. The changes in the scores were not monotonic. With linear and log quantization, the changes showed a slight plateau at $L = 12, 10$, and 8. The scores increased exponentially using small quantization step number of $L = 4$ or 6 with linear and log quantization, respectively. A pairwise t-test was used to test the significance of differences between the uncompressed and

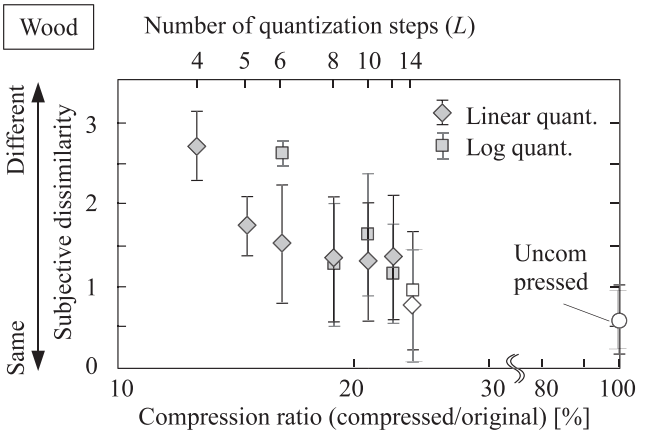

Fig. 7. Subjective dissimilarity between quantized and uncompressed wood texture. Filled symbols are significantly different from the uncompressed texture.

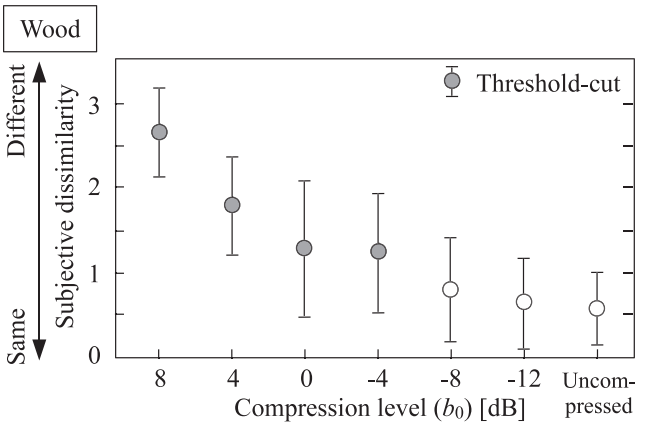

Fig. 8. Subjective dissimilarity between threshold-cut and uncompressed wood texture. Filled symbols are significantly different from the uncompressed texture.

compressed texture scores (Table 2). Significant increases were observed in the dissimilarity scores with both linear and log quantization for compression levels of 22.4 percent ($L = 12$) or less, as shown in the left and middle columns of the table.

Fig. 8 shows the means and standard deviations of the scores for the threshold-cut wood textures. The dissimilarity between the threshold-cut and uncompressed textures increased monotonically as the textures were compressed further with an increase in b_0, which was the size of the threshold curve shift. As shown in the right column of Table 2, textures compressed with a level of -4 dB had dissimilarity scores that were significantly different from the uncompressed texture.

Sandpaper. Fig. 9 shows the dissimilarity scores with the quantized sandpaper textures. A similar general trend was observed to that found with the wood textures, where the dissimilarity tended to increase as the compression ratio decreased. With linear quantization, the scores remained low when $L = 14 - 10$. However, the scores increased exponentially with small quantization steps. Table 3 shows the results of the statistical analysis of the scores for the sandpaper texture scores. With linear quantization, significant differences were observed between the scores of the uncompressed and compressed textures when the compression ratios were 22.4 and 18.8 percent or less, as shown in the left columns. With log quantization, significant differences in the scores were observed when the compression rates were below 20.8 percent, as shown in the middle columns.

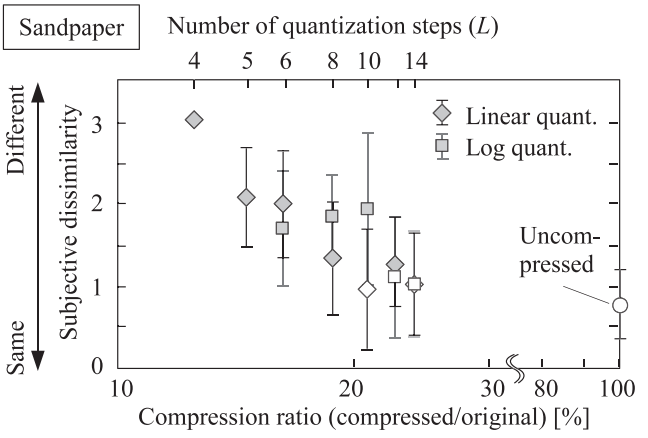

Fig. 9. Subjective dissimilarity between quantized and uncompressed sandpaper.

Fig. 10 shows the dissimilarity scores of the threshold-cut sandpapers. As found with wood textures, the scores increased almost monotonically as the compression level increased. Statistical tests showed that compressed textures where $b_0 = 0$ or greater produced significantly higher dissimilarity scores compared with the uncompressed textures as shown in the right columns of Table 3.

Leather. Fig. 11 shows the dissimilarity scores of the linearly quantized leather textures. In general, the dissimilarity scores increased with the compression of the texture. Quantized textures with $L = 4 - 6$ were highly dissimilar to uncompressed textures and the scores were high. Table 4 shows the results of statistical tests applied to the scores.

TABLE 2
Wood: t-Test to Compare the Results with Compressed and Uncompressed Wood Textures

Linear quantization				Log quantization				Threshold-cut		
Compress. level	Compress. ratio [%]	$t_0(9)$	p	Compress. level	Compress. ratio [%]	$t_0(9)$	p	Compress. level (dB)	$t_0(9)$	p
$L = 14$	23.8	0.946	0.369	$L = 14$	23.8	1.923	0.0867	$b_0 = -12$	0.394	0.703
$L = 12$	22.4	3.900	3.64E-3**	$L = 12$	22.4	3.541	6.30E-3**	$b_0 = -8$	1.283	0.232
$L = 10$	20.8	3.733	4.68E-3**	$L = 10$	20.8	5.612	3.29E-4**	$b_0 = -4$	3.616	5.61E-3**
$L = 8$	18.8	3.740	4.62E-3**	$L = 8$	18.8	3.585	5.89E-3**	$b_0 = 0$	3.387	8.04E-3**
$L = 6$	16.2	4.975	7.65E-4***	$L = 6$	16.2	23.32	2.33E-9***	$b_0 = 4$	7.413	4.05E-5***
$L = 5$	14.5	9.251	6.81E-6***					$b_0 = 8$	13.838	2.27E-7***
$L = 4$	12.5	15.93	6.69E-8***							

*, **, and *** indicate the significance levels of 0.05, 0.01, and 0.001, respectively.

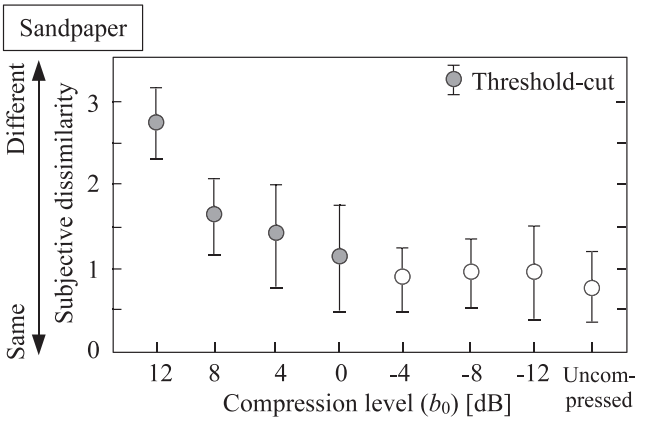

Fig. 10. Subjective dissimilarity between threshold-cut and uncompressed sandpaper.

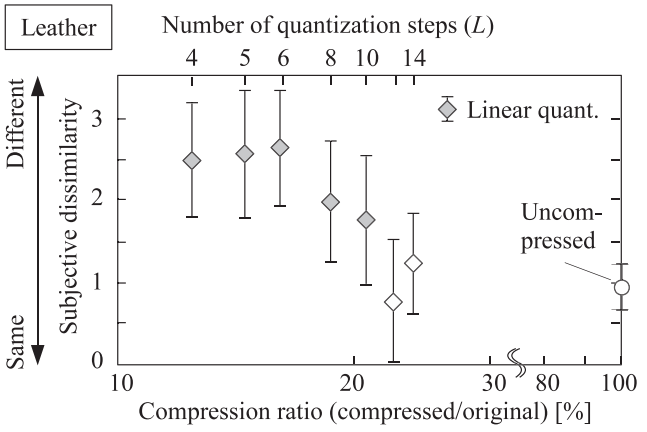

Fig. 11. Subjective dissimilarity between quantized and uncompressed leather.

The scores for the quantized leather textures were significantly higher than the uncompressed textures when the compression ratios were 20.8 percent ($L = 10$) or less, as shown in the left columns.

Fig. 12 shows the dissimilarity scores between the threshold-cut and uncompressed leather textures. The dissimilarity scores of the threshold-cut leather textures were not significantly different from the uncompressed texture when b_0 was -8 to 4 dB. The right columns of Table 4 show that significant differences among scores were observed with a compression level of $b_0 = 8$ and 12 dB.

5.4 Comparison with Sensitivity Index (d')

To validate the results obtained with grading scales, we obtained additional data using a discrimination task based on signal detection theory [40]. We report sensitivity index that is independent of participants response biases.

Task. Two of the participants were invited for additional experiments. They compared original (uncompressed) and compressed textures and answered whether or not they were the same. The experimental procedures were the same as those in Section 5.2.

Stimuli. The stimuli were the linearly quantized and threshold-cut textures in Table 1. The uncompressed textures were also included in the stimuli set. Each texture was presented 20 times for the individual participants. As a result, 280 (textures 14×20 repetitions), 300 (textures stimuli 15×20 repetitions), and 300 (textures 15×20 repetitions) trials were conducted for wood, sandpaper, and leather textures, respectively.

Results. We calculated d' values using the participants answers. Figs. 13 and 14 show the average d' values of the two participants for linearly quantized and threshold-cut textures, respectively. The filled symbols are the stimuli that were determined significantly different from the uncompressed ones using four point grading scales in the previous section. The values near symbols indicate their d' values.

TABLE 3
Sandpaper: t-Test to Compare the Results with Compressed and Uncompressed Sandpaper

Linear quantization				Log-quantization				Threshold-cut		
Compress. level	Compress. ratio [%]	$t_0(9)$	p	Compress. level	Compress. ratio [%]	$t_0(9)$	p	Compress. level (dB)	$t_0(9)$	p
$L = 14$	23.8	1.568	0.151	$L = 14$	23.8	1.756	0.113	$b_0 = -12$	1.152	0.279
$L = 12$	22.4	3.569	6.04E-3**	$L = 12$	22.4	1.940	0.084	$b_0 = -8$	1.378	0.202
$L = 10$	20.8	1.093	0.303	$L = 10$	20.8	5.195	5.68E-4***	$b_0 = -4$	1.006	0.341
$L = 8$	18.8	3.386	8.05E-3**	$L = 8$	18.8	7.467	3.82E-5***	$b_0 = 0$	2.270	0.0493*
$L = 6$	16.2	7.255	4.79E-5***	$L = 6$	16.2	5.228	5.43E-4***	$b_0 = 4$	3.840	3.97E-3**
$L = 5$	14.5	8.152	1.90E-5***					$b_0 = 8$	6.647	9.41E-5***
$L = 4$	12.5	25.57	1.03E-9***					$b_0 = 12$	15.26	9.73E-8***

TABLE 4
Leather: t-Test to Compare the Results with Compressed and Uncompressed Leather

Linear quantization				Threshold-cut		
Compress. level	Compress. ratio [%]	$t_0(9)$	p	Compress. level (dB)	$t_0(9)$	p
$L = 14$	23.8	1.954	0.0825	$b_0 = -12$	0.984	0.351
$L = 12$	22.4	0.995	0.346	$b_0 = -8$	0.267	0.796
$L = 10$	20.8	4.378	1.78E-3**	$b_0 = -4$	0.824	0.431
$L = 8$	18.8	5.947	2.16E-4***	$b_0 = 0$	0.335	0.745
$L = 6$	16.2	10.114	3.26E-6***	$b_0 = 4$	2.79E-15	1.00
$L = 5$	14.5	8.702	1.12E-5***	$b_0 = 8$	5.01	7.32E-4***
$L = 4$	12.5	9.078	7.96E-6***	$b_0 = 12$	6.94	6.76E-5***

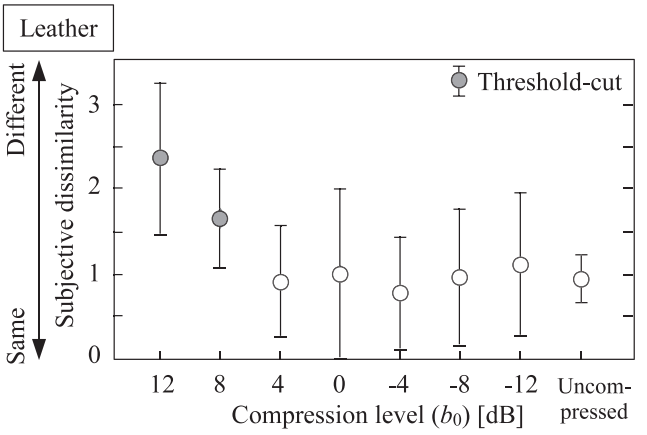

Fig. 12. Subjective dissimilarity between threshold-cut and uncompressed leather.

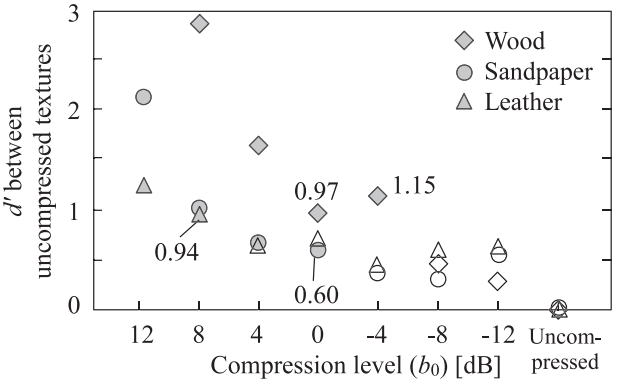

Fig. 14. d' values of threshold-cut textures: Filled symbols were significantly different from the uncompressed textures in accordance with four point grading scales.

The threshold levels determined using the grading scales, which were $L = 12$ for the wood and sandpaper and $L = 10$ for leather textures, corresponded to d' values of 0.67-0.87. For threshold-cut textures, the thresholds levels that were determined using grading scales, which were $b_0 = -4$, 0, and 8 dB for the wood, sandpaper, and leather textures, respectively, corresponded to d' values of 0.60-1.15. Thus, for both the linear quantization and threshold-cut algorithms, the threshold levels determined using grading scales were 0.6-1.15 in d' values.

In most psychophysical studies, $d' = 1$ is typically used as the performance criterion for defining a perception threshold. The thresholds obtained with grading scales were roughly consistent with those that would have been obtained by setting $d' = 1$ in a discrimination experiment using signal detection theory.

6 Discussion

6.1 Compression Ratios of Vibrotactile Material-Like Textures

Table 2 shows that participants reported no perceptual changes in quantized wood textures, even when the data size was compressed to 23.8 percent. Similarly, Tables 3 and 4 show that no perceptual changes were reported with compression of 23.8 and 22.4 percent for sandpaper and leather, respectively. These results indicate that vibrotactile material-like textures can be compressed to approximately 25 percent of the original data size by quantization, and they can be quantized using 12-14 steps. We suggest that a variety of textures can be compressed to this extent, because similar performances were observed with the three different types of texture.

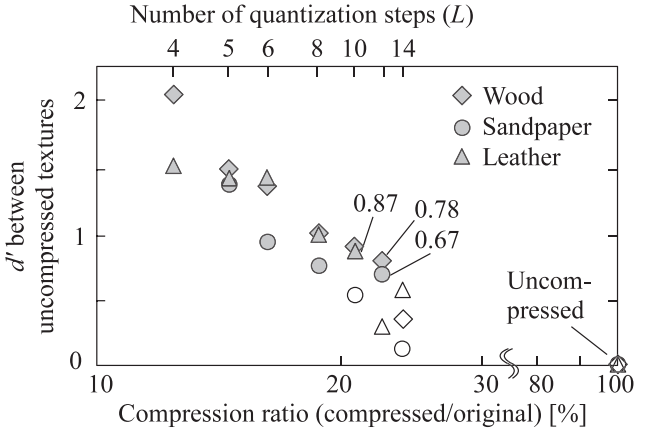

Fig. 13. d' values of linearly quantized textures: Filled symbols were significantly different from the uncompressed textures in accordance with four point grading scales.

The threshold-cut removed amplitudes lower than the shifted threshold curves. Thus, the amplitudes were truncated below the -8-dB, -4-dB, and 4-dB shifted curves for wood, sandpaper, and leather, respectively, while still maintaining the subjective similarity to the uncompressed textures. As a result, 28.7, 33.7, and 53.7 percent of data were assigned a value of zero with each type of textures. This is appropriate for lossless data compression algorithms such as Huffman encodings. Practical data compression methods are a combination of lossy and lossless data compression schemes. We applied the Huffman encoding [16] to the quantized textures, as shown in Table 5. The table indicates that linear quantization coupled with Huffman encoding reduced the data size to 22.3, 17.5, and 12.1 percent for the wood, sandpaper, and leather textures, respectively, excluding the data size of decoding trees or tables.

In summary, the quantization and threshold-cut methods were effective for the lossy data compression of vibrotactile textures. The application of linear quantization alone decreased the data sizes to approximately 25 percent of the original size while maintaining the perceptual quality of textures. A combination with a lossless scheme resulted in more efficient compression of textures. The performances of these methods were confirmed using single type of vibrotactile display and a limited variety of texture stimuli.

TABLE 5
Compression Ratios Achieved by a Combination with Huffman Coding

	Compression ratio (compressed/uncompressed) [%]	
	Linear quant. only	Linear quant. + Huffman
Wood	23.8% ($L = 14$)	22.3%
Sandp.	23.8% ($L = 14$)	17.5%
Leather	22.4% ($L = 12$)	12.1%

In the future, compression algorithms will be evaluated against other types of vibrotactile displays and textures.

6.2 Subthreshold Data Should NOT be Automatically Removed

We assumed the perception of vibrotactile textures was not affected by the deletion of frequency components with amplitudes below the perceptual thresholds. However, the experimental results did not support this assumption. A threshold-cut algorithm with $b_0 = 0$ dB removed the amplitudes below the perceptual thresholds, but the participants detected differences between the threshold-cut and original textures of wood and sandpaper textures under these conditions. Perceptual changes in wood textures were also reported when the algorithm truncated amplitudes lower than a -4-dB shifted threshold. Thus, the subthreshold amplitudes should not be automatically removed.

A possible major reason for this phenomenon was that the threshold curve used by the algorithm was for single frequency vibratory stimuli. It is known that subliminal noise could help the perception of vibrotactile stimuli [41], [42]. Hence, the deletion of amplitudes below the perceptual thresholds by information compression may affect the perception of vibrotactile textures. In contrast, we should note that the perceptual thresholds could be raised by some reasons. In such cases, the stimuli below the threshold levels are less likely to influence the perception of textures. For example, noisy vibratory stimuli increase the perceptual thresholds of receptive units when the sensitive frequency bands are located in the noise frequency [35], [43]. Furthermore, hand movements could affect the thresholds. The threshold curve used in this study was acquired when the hand was held still; however, voluntary hand movements could elevate the perceptual thresholds of vibratory stimuli applied to fingers [44].

The differences between the results for materials can be attributed to the differences in frequency components included in each material. Bensmaïa et al. attempted to explain the subjective similarity between two fine textures on the basis of the similarity of frequency spectra of skin vibrations caused by stroking them [36], [37]. They claimed that the effect of vibratory power on the subjective quality of textures varied with frequency bands. Some frequency bands significantly influence the quality whereas the others do not. It is likely that the deletion of these minor frequencies does not affect quality change. Thus, the valid compression levels of threshold-cut are possibly dependent on the frequency spectra of material textures; however, it seems that the psychological aspects for quantitatively discussing this possibility have not been sufficiently considered thus far.

6.3 Quantization Nonmonotonically Changes the Similarity

In general, the compression made textures dissimilar to the original ones. Hence, Figs. 7, 8, 9, 10, 11, and 12 show the downward slopes. However, as exceptions, some compressed textures resembled the original ones. For example, for the linear quantization of the wood texture, the dissimilarity at $L = 8$ (square in Fig. 7) was unexpectedly small. Further, $L = 10$ for sandpaper (diamond in Fig. 9) and $L = 12$ for leather (Fig. 11) were these exceptions. These exceptional phenomena were prominent with the quantization algorithms rather than with the threshold-cut algorithm. We speculate that this was due to the changes in stimuli energies. In the threshold-cut algorithm, the energy of the stimuli decreased with the compression ratio. Hence, when textures were compressed further, they became more dissimilar to the original ones. In contrast, quantization could increase the stimuli energy. This increase might have unexpectedly made the compressed textures similar to the original ones. Bensmaïa et al. reported that the sum of weighted power spectrum of vibrotactile stimulus possibly determined the quality of stimuli [36], [37]. Even when the spectra of two stimuli were different, these stimuli could be perceptually close if their sums of weighted spectra were close.

6.4 Limitation of Current Approaches

Although this study confirmed the effectiveness of lossy data compression of vibrotactile material-like textures, the current algorithms have a problem in assuming the hand velocity. We computed the frequency spectra of vibrotactile stimuli on the basis of a constant hand velocity of 50 mm/s. However, it originally depends on individuals. This means that the tactile stimuli presented to users depend on their exploratory hand speeds. Unlike visual or audio signals, the required sampling rate and compression ratio for texture data also depends on individual users or their hand velocities. The algorithms are not necessarily optimal for users who explore virtual textures at speeds significantly different from the supposed average speed. The problem of user dependency seems to be unique to haptic content; it is necessary to investigate and develop compression algorithms independent of hand velocities.

7 Conclusion

We studied the applicability and appropriate compression ratios for lossy data compression of vibrotactile material-like textures. In particular, we focused on the use of quantization and the truncation of subthreshold signals as compression schemes. We tested these methods using a vibrotactile display and three types of material surface roughness patterns. In a series of psychological experiments, participants compared compressed and uncompressed textures and rated their differences or similarities. We used these results to identify the best compression levels that did not lead to perceptual quality changes. We found that quantization was significantly effective for this purpose. Spectral amplitudes of the vibrotactile textures were linearly quantized using approximately 14 steps, which reduced the data size to less than the 25 percent of the original data. We also found that the truncation of frequency components below a shifted perceptual threshold curve was effective. However, it was shown that subthreshold amplitudes should not be automatically removed and a shifted curve should be applied. The amount of shift depended on the type of texture, but it was expected to range from -8 to 4 dB. A combination of these two lossy compression schemes with Huffman coding can potentially

enable considerable reduction in data size. Further studies on this topic can contribute to the availability of haptic content on the Internet.

ACKNOWLEDGMENTS

This work was supported in part by MEXT KAKENHI (23135514).

REFERENCES

[1] Y. Ikei, K. Wakamatsu, and S. Fukuda, "Vibratory Tactile Display of Image-Based Textures," *IEEE Computer Graphics and Applications,* vol. 17, no. 6, pp. 53-61, Nov./Dec. 1997.

[2] D.G. Caldwell, N. Tsagarakis, and C. Giesler, "An Integrated Tactile/Shear Feedback Array for Stimulation of Finger Mechanoreceptor," *Proc. IEEE Int'l Conf. Robotics and Automation,* pp. 287-292, 1999.

[3] M. Konyo, S. Tadokoro, and T. Takamori, "Artificial Tactile Feel Display Using Soft Gel Actuators," *Proc. IEEE Int'l Conf. Robotics and Automation,* vol. 4, pp. 3416-3421, 2000.

[4] D. Allerkamp, G. Bottcher, F.-E. Wolter, A.C. Brady, J. Qu, and I.R. Summers, "A Vibrotactile Approach to Tactile Rendering," *Visual Computer,* vol. 23, pp. 97-108, 2007.

[5] L. Winfield, J. Glassmire, E.J. Colgate, and M. Peshkin, "T-pad: Tactile Pattern Display through Variable Friction Reduction," *Proc. World Haptics Conf.,* pp. 421-426, 2007.

[6] M. Fukumoto and T. Sugimura, "Active Click: Tactile Feedback for Touch Panels," *Proc. ACM SIGCHI Conf. Human Factors in Computing Systems,* pp. 121-122, 2001.

[7] I. Poupyrev, S. Maruyama, and J. Rekimoto, "Ambient Touch: Designing Tactile Interface for Handheld Device," *Proc. 15th Ann. ACM Symp. User Interface Software and Technology,* pp. 51-60, 2002.

[8] A. Nashel and S. Razzaque, "Tactile Virtual Buttons for Mobile Devices," *Proc. ACM SIGCHI Conf. Human Factors in Computing Systems,* pp. 854-855, 2003.

[9] J.C. Lee, P.H. Dietz, D. Leigh, W.S. Yerazunis, and S.E. Hudson, "Haptic Pen: A Tactile Feedback Stylus for Touch Screens," *Proc. 17th Ann. ACM Symp. User Interface Software and Technology,* pp. 291-294, 2004.

[10] J. Luk, J. Pasquero, S. Little, K.E. MacLean, V. Levesque, and V. Hayward, "A Role for Haptics in Mobile Interaction: Initial Design Using a Handheld Tactile Display Prototype," *Proc. ACM Conf. Human Factors in Computing Systems,* pp. 171-180, 2006.

[11] S. Brewster, "Tactile Feedback for Mobile Interactions," *Proc. ACM SIGCHI Conf. Human Factors in Computing Systems,* pp. 159-162, 2007.

[12] A.M. Okamura, M.R. Cutkosky, and J.T. Dennerlein, "Reality-Based Models for Vibration Feedback in Virtual Environments," *IEEE/AME Trans. Mechatronics,* vol. 6, no. 3, pp. 245-252, Sept. 2001.

[13] M. McMahan and K. Kuchenbecker, "Haptic Display of Realistic Tool Contact via Dynamically Compensated Control of a Dedicated Actuator," *Proc. IEEE/RSJ Int'l Conf. Intelligent Robots and Systems,* pp. 3170-3177, 2009.

[14] L.M. Brown, A. Sellen, R. Krishna, and R. Harper, "Exploring the Potential of Audio-Tactile Messaging for Remote Interpersonal Communication," *Proc. 27th ACM Conf. Human Factors in Computing Systems,* pp. 1527-1530, 2009.

[15] Y. Hashimoto and H. Kajimoto, "A Novel Interface to Present Emotional Tactile Sensation to a Palm Using Air Pressure," *Proc. SIGCHI Conf. Human Factors in Computing Systems,* pp. 2703-2708, 2008.

[16] K.R. Rao and J.J. Hwang, *Techniques and Standards for Image, Video, and Audio Coding.* Prentice Hall, 1996.

[17] I.R. Summers and C.M. Chanter, "A Broadband Tactile Array on the Fingertip," *J. Acoustical Soc. Am.,* vol. 112, no. 5, pp. 2118-2126, 2002.

[18] J. Pasquero, J. Luk, V. Lévesque, Q. Wang, V. Hayward, and K.E. MacLean, "Haptically Enabled Handheld Information Display with Distributed Tactile Transducer," *IEEE Trans. Multimedia,* vol. 9, no. 4, pp. 746-753, June 2007.

[19] S. Okamoto and Y. Yamada, "Perceptual Properties of Vibrotactile Material Texture: Effects of Amplitude Changes and Stimuli Beneath Detection Thresholds," *Proc. IEEE/SICE Int'l Symp. System Integration,* pp. 384-389, 2010.

[20] T. Tada, K. Cho, H. Shimoda, T. Sakata, and S. Sobue, "An Evaluation of JPEG Compression for On-Line Satellite Images Transmission," *Proc. Int'l Geoscience and Remote Sensing Symp.,* vol. 3, pp. 1515-1518, 1993.

[21] K.R. Persons, N.J. Hangiandreou, N.T. Charboneau, J.W. Charboneau, E.M. James, B.R. Douglas, A.P. Salmon, J.M. Knudsen, and B.J. Erickson, "Evaluation of Irreversible JPEG Compression for a Clinical Ultrasound Practice," *J. Digital Imaging,* vol. 15, no. 1, pp. 15-21, 2005.

[22] P. Hinterseer and E. Steinbach, "Psychophysically Motivated Compression of Haptic Data," *Proc. Joint Int'l COE/HAM-SFB453 Workshop Human Adaptive Mechatronichs and High Fidelity Telepresence,* pp. 19-23, 2005.

[23] S. Hirche, P. Hinterseer, E. Steinbach, and M. Buss, "Transparent Data Reduction in Networked Telepresence and Teleaction Systems. Part i: Communication without Time Delay," *Presence,* vol. 16, no. 5, pp. 523-531, 2007.

[24] V. Nitsch, J. Kammerl, B. Faerber, and E. Steinbach, "On the Impact of Haptic Data Reduction and Feedback Modality on Quality and Task Performance in a Telepresence and Teleaction System," *Proc. Int'l Conf. Haptics: Generating and Perceiving Tangible Sensations (EuroHaptics),* pp. 169-176, 2010.

[25] V. Nitsch, B. Färber, L. Geiger, P. Hinterseer, and E. Steinbach, "An Experimental Study of Lossy Compression in a Real Telepresence and Teleaction System," *Proc. IEEE Int'l Workshop Haptic Audio Visual Environments and Their Applications,* pp. 75-80, 2008.

[26] C. Shahabi, A. Ortega, and M.R. Kolahdouzan, "A Comparison of Different Haptic Compression Techniques," *Proc. IEEE Int'l Conf. Multimedia and Expo,* vol. 1, pp. 657-660, 2002.

[27] Y. You and M.Y. Sung, "Haptic Data Transmission Based on the Prediction and Compression," *Proc. Int'l Conf. Comm.,* pp. 1824-1828, 2008.

[28] M. Kuschel, P. Kremer, S. Hirche, and M. Buss, "Lossy Data Reduction Methods for Haptic Telepresence Systems," *Proc. IEEE Int'l Conf. Robotics and Automation,* pp. 2933-2938, 2006.

[29] N. Jensen, G. Gaus, G. von Voigt, and S. Olbrich, "Design and Psychophysical Study of Volume Compression for Haptic Rendering," *Proc. Second Joint EuroHaptics Conf. and Symp. Haptic Interfaces for Virtual Environment and Teleoperator Systems,* pp. 261-267, 2007.

[30] I. Arimoto, K. Hikichi, H. Morino, K. Sezaki, and Y. Yasuda, "Data Compression for Haptic Communication System (in Japanese)," technical report of the IEICE, vol. DSP2001-147, pp. 17-22, 2001.

[31] C.W. Borst, "Predictive Coding for Efficient Host-Device Communication in a Pneumatic Force-Feedback Display," *Proc. IEEE First Joint Eurohaptics Conf. and Symp. Haptic Interfaces for Virtual Environment and Teleoperator Systems (WorldHaptics),* pp. 596-599, 2005.

[32] S.A. Cholewiak, K. Kim, H.Z. Tan, and B.D. Adelstein, "A Frequency-Domain Analysis of Haptic Gratings," *IEEE Trans. Haptics,* vol. 3, no. 1, pp. 3-14, Jan.-Mar. 2010.

[33] S.J. Bensmaïa and M. Hollins, "Complex Tactile Waveform Discrimination," *J. Acoustical Soc. Am.,* vol. 108, pp. 1236-1245, 2000.

[34] J.C. Craig, "Difference Threshold for Intensity of Tactile Stimuli," *Perception & Psychophysics,* vol. 11, no. 2, pp. 150-152, 1972.

[35] G.A. Gescheider, S.J. Bolanowski, J.J. Zwislocki, K.L. Hall, and C. Mascia, "The Effects of Masking on the Growth of Vibrotactile Sensation Magnitude and on the Amplitude Difference Limen: A Test of the Equal Sensation Magnitude-Equal Difference Limen Hypothesis," *J. Acoustical Soc. Am.,* vol. 96, no. 3, pp. 1479-1488, 1994.

[36] S. Bensmaïa and M. Hollins, "Pacinian Representations of Fine Surface Texture," *Perception & Psychophysics,* vol. 67, no. 5, pp. 842-854, 2005.

[37] S. Bensmaïa, M. Hollins, and J. Yau, "Vibrotactile Intensity and Frequency Information in the Pacinian System: A Psychophysical Model," *Perception & Psychophysics,* vol. 67, no. 5, pp. 828-841, 2005.

[38] M. Wiertlewski, J. Lozada, and V. Hayward, "The Spatial Spectrum of Tangential Skin Displacement Can Encode Tactual Texture," *IEEE Trans. Robotics,* vol. 27, no. 3, pp. 461-472, June 2011.

[39] *Recommendation ITU-R BT.500-12, Methodology for the Subjective Assessment of the Quality of Television Pictures,* Int'l Telecomm. Union, 2009.

[40] N.A. Macmillan and C.D. Creelman, *Detection Theory - A User's Guide*, second ed. Psychology Press, 2009.
[41] J.J. Collins, T.T. Imhoff, and P. Grigg, "Noise-Enhanced Tactile Sensation," *Nature*, vol. 383, p. 770, 1996.
[42] C. Wells, L.M. Ward, R. Chua, and J.T. Inglis, "Touch Noise Increases Vibrotactile Sensitivity in Old And Young," *Psychological Science*, vol. 16, no. 4, pp. 313-320, 2005.
[43] G.A. Gescheider, R.T. Verrillo, and C.L. Van Doren, "Prediction of Vibrotactile Masking Functions," *J. Acoustical Soc. Am.*, vol. 72, no. 5, pp. 1421-1426, 1982.
[44] P. Dyhre-Poulsen, "Perception of Tactile Stimuli before Ballistic and during Tracking Movements," *Active Touch*, G. Gordon, ed., Pergamon Press, pp. 171-176, 1978.

Shogo Okamoto (M '06) received the BS degree in engineering from Kobe University in 2005, and the MS and PhD degrees in information sciences in 2007 and 2010, respectively, from the Graduate School of Information Sciences, Tohoku University. Since 2010, he has been an assistant professor in the Graduate School of Engineering, Nagoya University. His research interests include haptic interfaces and human factors. He is a member of the IEEE.

Yoji Yamada received the PhD degree from the Tokyo Institute of Technology, Japan, in 1990. He had been an associate professor at Toyota Technological Institute. In 2004, he joined the National Institute of Advanced Industrial and Science Technology (AIST) as a group leader of Safety Intelligence Research Group. In 2009, he joined the Department of Mechanical Science and Engineering, Graduate School of Engineering, Nagoya University as a professor. He is a member of the IEEE.